ASSESSING DELAMINATION INITIATION FROM FIBER AND MATRIX PROPERTIES

Zheng-Ming Huang[1], Jia-Jie Gu[2]

[1]Tongji University, 1239 Siping Road, Shanghai 200092, China. huangzm@tongji.edu.cn

[2]Tongji University, 1239 Siping Road, Shanghai 200092, China. gujiajie@tongji.edu.cn

Keyword: Laminate; delamination initiation; Bridging model; Micromechanics; Stress concentration factors

ABSTRACT

Delamination generally occurs due to an edge effect. As the laminate is essentially bonded together form the individual laminate by the matrix, any delamination of the laminate must be initiated from a matrix failure and thus controlled by the stresses of the matrix. Based on this viewpoint, this paper predicts the initiation of laminate delamination through analyzing the stresses of the matrix. The stress field of a symmetrically laminated plate under an axial load is calculated by a three-dimensional finite element approach. To deal with the weak singularity occurred in the interlaminar stresses at the free edge, an average for the stresses of each lamina with respect to its thickness is carried out, and the internal stresses in the fiber and matrix of the lamina are determined in terms of the Bridging micromechanics Model. The thus obtained homogenized internal stresses must be converted into "true" values before a failure assessment can be made with respect to the original strength data of the fiber and matrix. Whereas the true stresses of the fiber are the same as its homogenized ones, those of the matrix are obtained by multiplying its homogenized quantities by respective stress concentration factors (SCFs) of the matrix in the composite. Such an SCF cannot be defined following a classical approach. All of the SCFs with perfect interface bonding and the transverse tensile SCF with a debonded interface have been calculated. Finally, an in-plane failure and a delamination initiation are considered separately for the laminate. The most important feature of this work is in that only the original elastic and strength data of the fiber and matrix are required in the prediction of a delamination initiation. Our predictions correlate reasonably with the available experimental data.

1 INTRODUCTION

Near the free-edge of a laminated composite under an axial load, the stress state has to be a three dimensional one in order to satisfy boundary condition. So the plane stress assumption used in Classical Laminate Theory (CLT) is no longer valid. There are many approaches to calculate the interlaminar stresses, i.e. finite difference method[1], 3D finite element method[2], boundary layer technique and multi-particle model. The interlaminar stresses at the free-edge can cause delamination between lamina plies, which may degrade properties of the laminate and induce an earlier ultimate failure. In applications, delamination is one of the most common failure mechanisms in a laminated composite. Delamination is consisted of an initiation and growth process. Once the initiation happens, the delamination may undergo a stable crack growth until an ultimate failure occurs. Thus, an efficient method for predicting an initiation of delamination is needed. A stress failure criterion involving an average of the interfacial stresses over a characteristic length from the edge is often proposed to predict the initiation of delamination, which addresses the problem resulted from a stress singularity at the free edge. But, there is not yet a general rule to determine the characteristic length. Kim and Soni[3] set it equal to the ply thickness, whereas Brewer and Lagace[4] deemed that the characteristic length should be extracted from experiments. Lorrit[5] proposed a procedure to determine the characteristic length, which still requires the test results of the laminate. There are also energy based approaches to a delemination initiation, in which the interfacial strain energy release rate and the size of the effective flaw may be needed[6]. Martin and Leguillon[7] combined a strength and an energy approaches. They thought that a delamination would occur when the strength and the energy conditions were met simultaneously.

Most of the existing methods for a delamination initiation are phenomenological. Little has been found in the literature to approach it from a viewpoint of micromechanics. As a laminate is essentially bonded together form the individual laminae by the matrix, any delamination of the laminate must be initiated from a matrix failure and thus controlled by the stresses of the matrix. In this study an attempt has been made to predict an initiation of delamination through the stresses of the matrix, which are calculated by a combined finite element approach (FEA) and the Bridging micromechanics Model. And then a stress failure criterion only involving the stresses and the original strengths of the matrix has been applied to predict a delamination threshold load. The predicted data are compared with experimental results for a variety of laminates.

2 FINITE ELEMENT MODEL

Consider a plate of different laminates under a uniform axial extension. The laminates have the following dimensions: length L=40mm, width b=15mm, and varied thicknesses. Global coordinates x, y and z correspond to the length, width and the thickness directions, respectively. Supposing the laminates are symmetric with respect to the x-y plane at z=0, the analysis can be performed only for the upper half of the laminates. **Figure 1** shows a laminate geometry and the global coordinate system. A tension of σ_x is applied along the x direction on the face at $x=L$. The boundary conditions as follows:

$$u(0,y,z)=0,\ v(0,0,0)=0,\ w(x,y,0)=0$$

where u, v, and w are the displacements of the laminate along the x, y, and z directions, respectively.

The material system used is T800 carbon fiber and 914 epoxy matrix[5]. No constituent properties were provided in Ref. [5]. Instead, the mechanical properties of the unidirectional (UD) composite from this system, given in [5] and shown in **Table 1**, are able to match with those made from the IM7 fiber and 914-C matrix provided in [8]. Thus, the original elastic and strength parameters of the T800 fiber and 914 matrix are assigned as those of the IM7 fiber and 914-C matrix, as listed in **Table 2**[8]. It is noted that a fiber volume fraction of V_f=0.55 was also adjusted in such a way that the predicted properties of the UD composite from **Table 2** were close to those shown in **Table 1**.

Mechanical characteristics	E_{11} (GPa)	E_{22} (GPa)	G_{12} (GPa)	υ_{12}	X (MPa)	Y (MPa)	S (MPa)
value	159	8.4	4.1	0.33	2400	50	100

Table 1: Mechanical properties of a T800/914 UD composite[5]

	E_{11} (Gpa)	E_{22} (Gpa)	ν_{12}	G_{12} (Gpa)	ν_{23}	$\sigma_{u,t}$ (Mpa)	$\sigma_{u,c}$ (Mpa)	$\sigma_{u,s}$ (Mpa)	V
Fiber	276	19	0.2	27	0.36	5180	3200	-	0.55
Matrix	4	4	0.35	1.481	0.35	75	150	70	0.45

Table 2: Mechanical properties of T800 fiber and 914 matrix[8]

The FEA is carried out through ABAQUS. An 8-node solid element (C3D8R) is chosen for the analysis. There are 136 elements in the y-direction, which are gradually refined to the free edge. Choosing $[\pm 10]_s$ laminate as an example, a convergence study has been performed by increasing the element number in the thickness direction of each layer. The interlaminar stress component, σ_{xz}, obtained by using 2 to 10 elements in the thickness of a ply are plotted in **Figure 2** and **figure 3**, in which the Lorrit's solution is also shown. It is seen that the interlaminar stress at the free edge is dependent on the mesh number. In other words, there is a singularity at the free edge, and the maximum interlaminar stress near the free edge is meaningless. This kind of singularity can be solved by taking an average on the stresses of each lamina with respect to its thickness. **Figure 4** shows the averaged stress distributions *vs* mesh number used along the ply thickness. From the figure, it can conclude that the averaged interlaminar stress is constant as long as the element number in the thickness is equal to or greater than 2.

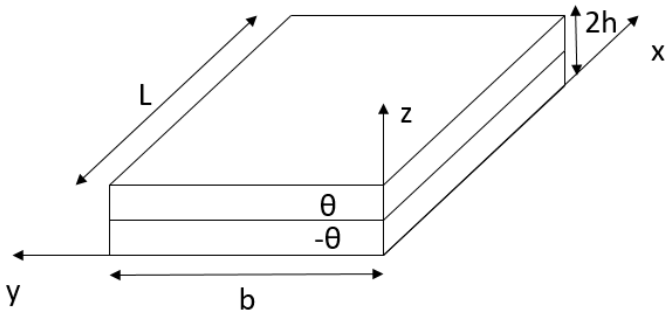

Figure 1: Upper half of the laminate $[\pm\theta]_s$ used in a FEA

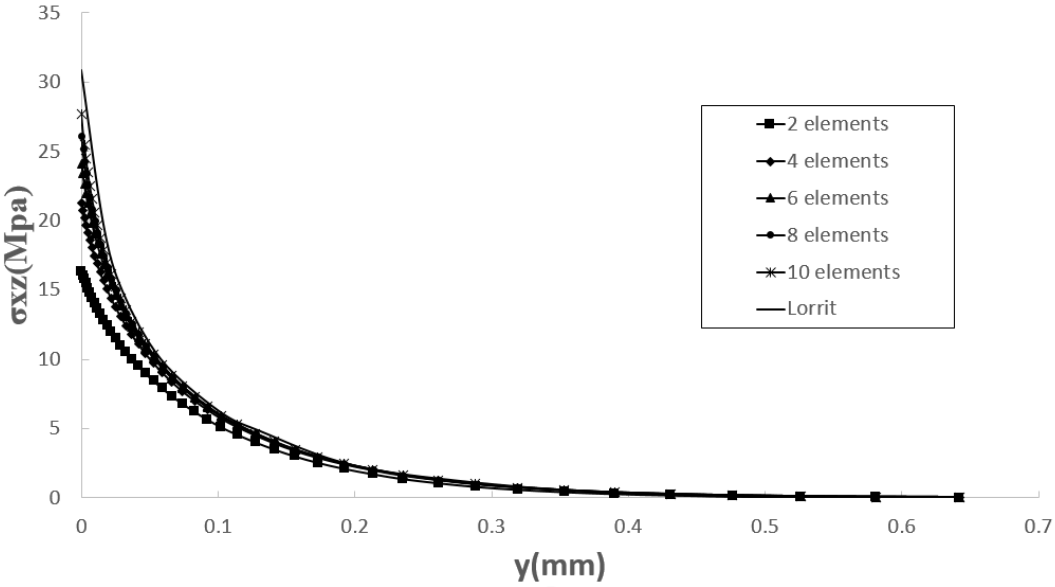

Figure 2: interlaminar stress σ_{xz} at z=h in T800/914 [±10]s laminates versus y for different numbers of elements through thickness for each layer

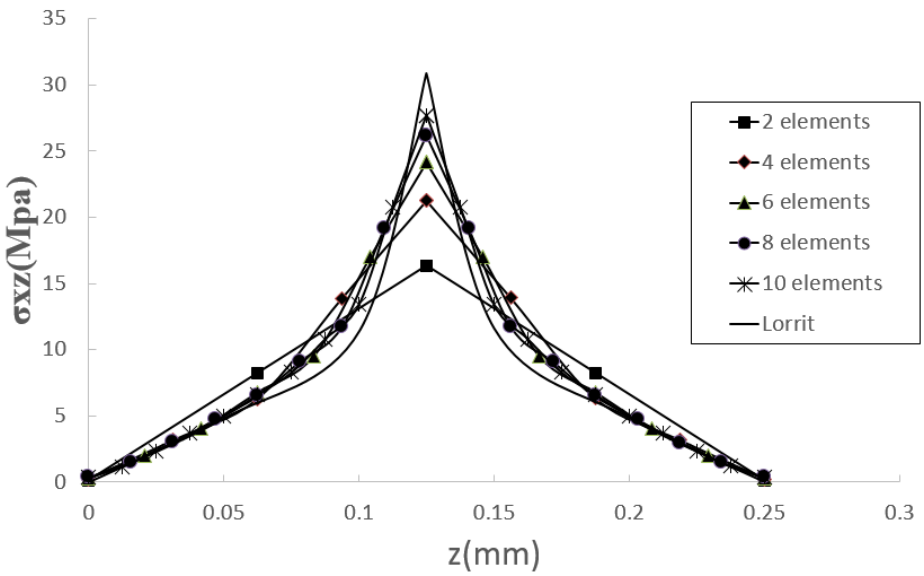

Figure 3: interlaminar stress σ_{xz} at y=b in T800/914 [±10]s laminates versus z for different numbers of elements through thickness for each layer

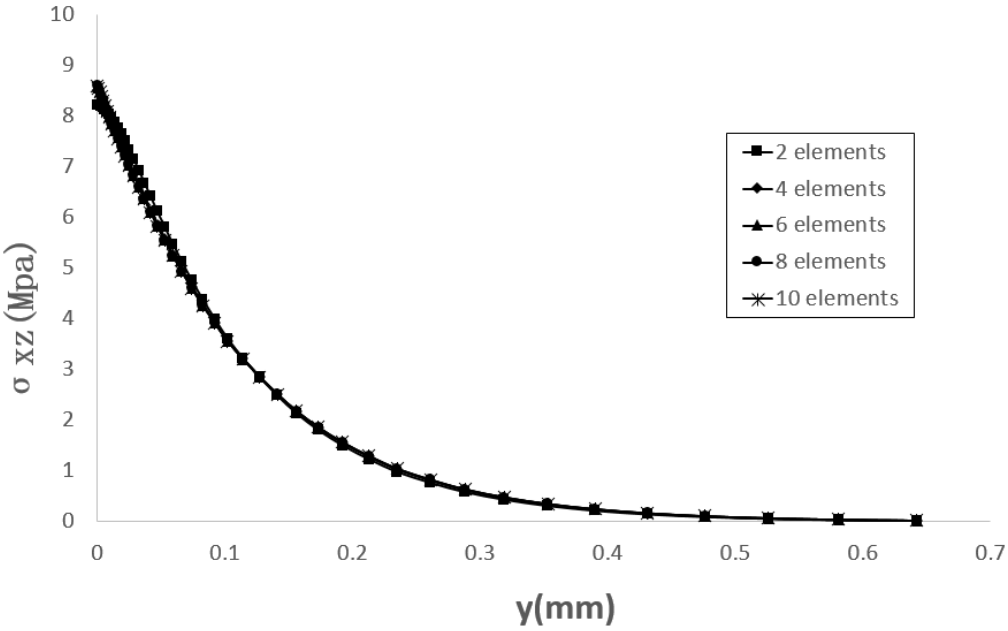

Figure 4: average interlaminar stress σ_{xz} in -10 ply versus y for different numbers of elements through thickness for each layer

3 INTERNAL STRESS DETERMINATION

As the laminate is essentially bonded together from the individual laminate by the matrix, any delamination of the laminate must be initiated from a matrix failure and thus controlled by the stresses of the matrix. To determine the internal stresses in the fiber and matrix, the stress increments at any point of a special lamina of the laminate, $\{d\sigma\}^G = \{d\sigma_{xx}, d\sigma_{yy}, d\sigma_{zz}, d\sigma_{yz}, d\sigma_{xz}, d\sigma_{xy}\}^T$, which are calculated by the finite element method in the global coordinate system, are transformed into those in the lamina local system, $\{d\sigma\} = \{d\sigma_{11}, d\sigma_{22}, d\sigma_{33}, d\sigma_{23}, d\sigma_{13}, d\sigma_{12}\}^T$, through (**Figure 5**)

$$\{d\sigma\} = \left[T_{\mathrm{ij}}\right]_{\mathrm{c}}^{-1}\{d\sigma\}^G, \tag{1.1}$$

$$[T_{\mathrm{ij}}]_{\mathrm{c}} = \begin{bmatrix} l_1^2 & l_2^2 & l_3^2 & 2l_2l_3 & 2l_1l_3 & 2l_2l_1 \\ m_1^2 & m_2^2 & m_3^2 & 2m_2m_3 & 2m_3m_1 & 2m_1m_2 \\ n_1^2 & n_2^2 & n_3^2 & 2n_2n_3 & 2m_3m_1 & 2m_1m_2 \\ m_1n_1 & m_1n_2 & m_3n_3 & m_2n_3+m_3n_2 & n_3m_1+n_1m_3 & m_1n_2+m_2n_1 \\ n_1l_1 & n_2l_2 & n_2l_2 & l_2n_3+l_3n_2 & n_3l_1+n_1l_3 & l_1n_2+l_2n_1 \\ l_1m_1 & l_2m_2 & l_3m_3 & l_2m_3+l_3m_2 & m_3l_1+m_1l_3 & l_1m_2+l_2m_1 \end{bmatrix}, \tag{1.2}$$

with l_i=cos(x, x_i), m_i=cos(y, x_i), and n_i=cos(z, x_i). Suppose that the fiber and matrix are linearly elastic until rupture. The internal stress increments in the fiber and matrix of each lamina are determined in terms of the Bridging micromechanics Model as

$$\{d\sigma_i^f\} = (V_f[I] + V_m[A_{ij}])^{-1}\{d\sigma_j\}, \tag{2}$$

$$\{d\sigma_i^m\} = [A_{ij}](V_f[I] + V_m[A_{ij}])^{-1}\{d\sigma_j\}, \tag{3}$$

$$[A_{ij}] = \begin{bmatrix} A_{11} & A_{12} & A_{13} & 0 & 0 & 0 \\ 0 & A_{22} & 0 & 0 & 0 & 0 \\ 0 & 0 & A_{33} & 0 & 0 & 0 \\ 0 & 0 & 0 & A_{44} & 0 & 0 \\ 0 & 0 & 0 & 0 & A_{55} & 0 \\ 0 & 0 & 0 & 0 & 0 & A_{66} \end{bmatrix}, \tag{4.1}$$

$$A_{11} = \frac{E^{\mathrm{m}}}{E_{11}^{f}}, \tag{4.2}$$

$$A_{22} = A_{33} = A_{44} = 0.3 + 0.7\frac{E^{\mathrm{m}}}{E_{22}^{f}}, \tag{4.3}$$

$$A_{55} = A_{66} = 0.3 + 0.7\frac{G^{\mathrm{m}}}{G_{12}^{f}}, \tag{4.4}$$

$$A_{12} = A_{13} = \frac{S_{12}^{\mathrm{f}} - S_{12}^{\mathrm{m}}}{S_{11}^{\mathrm{f}} - S_{11}^{\mathrm{m}}}(A_{11} - A_{22}) = \frac{\nu^{m}E_{11}^{f} - E^{m}\nu_{12}^{f}}{E^{m} - E_{11}^{f}}(A_{11} - A_{22}). \tag{4.5}$$

E_{11}^{f}, E_{22}^{f}, and G_{12}^{f} are, respectively, the longitudinal, transverse, and in-plane shear moduli of the fiber, and ν_{12}^{f} is its longitudinal Poisson's ratio. E^m and ν^m are the Young's modulus and Poisson's ratio of the matrix, respectively.

The internal stresses calculated by the bridging model are homogenized quantities. They must be converted into true values before a failure detection for the fiber and matrix can be made against their original strength data. Whereas the stress field in the fiber of a composite is uniform, meaning that the homogenized and the true stresses of the fiber are the same, the one in the matrix is not uniform. The matrix's true stresses are obtained by multiplying the homogenized quantities with respective stress concentration factors (SCFs) of the matrix in the composite. The current interlaminar stresses of the matrix are simply updated through

$$(\bar{\sigma}_{11}^{m})_{k+1} = (\bar{\sigma}_{11}^{m})_{k} + d\sigma_{11}^{m}, \tag{5.1}$$

$$(\bar{\sigma}_{22}^{m})_{k+1} = (\bar{\sigma}_{22}^{m})_{k} + K_{22}d\sigma_{22}^{m}, \tag{5.2}$$

$$(\bar{\sigma}_{33}^{m})_{k+1} = (\bar{\sigma}_{33}^{m})_{k} + K_{33}d\sigma_{33}^{m}, \tag{5.3}$$

$$(\bar{\sigma}_{23}^{m})_{k+1} = (\bar{\sigma}_{23}^{m})_{k} + K_{23}d\sigma_{23}^{m}, \tag{5.4}$$

$$(\bar{\sigma}_{13}^{m})_{k+1} = (\bar{\sigma}_{13}^{m})_{k} + K_{13}d\sigma_{23}^{m}, \tag{5.5}$$

$$(\bar{\sigma}_{12}^{m})_{k+1} = (\bar{\sigma}_{12}^{m})_{k} + K_{12}d\sigma_{12}^{m}, \tag{5.6}$$

where K_{ij} are the SCFs of the matrix corresponding to different loads and different interface bonding conditions with the fiber. Supposing that $d\sigma_{22}^{m}$ and $d\sigma_{33}^{m}$ do not occur simultaneously, we have

$$K_{22} = K_{33} = \begin{cases} K_{33}^{t}, if\ d\sigma_{22}^{m}(or\ d\sigma_{33}^{m}) > 0\ and\ (\bar{\sigma}_{e}^{m})_{k} < \hat{\sigma}_{e}^{m} \\ \hat{K}_{33}^{t}, if\ d\sigma_{22}^{m}(or\ d\sigma_{33}^{m}) > 0\ and\ (\bar{\sigma}_{e}^{m})_{k} \geq \hat{\sigma}_{e}^{m}\ \ \&\ (\bar{\sigma}_{m}^{1})_{k} > 0 \\ K_{33}^{c}, if\ d\sigma_{22}^{m}(or\ d\sigma_{33}^{m}) < 0 \end{cases}, \tag{6}$$

If both $d\sigma_{22}^{m}$ and $d\sigma_{33}^{m}$ exist, the situation will be more complicated. The parameters in Eq. (6) are as follows.

$$K_{33}^{t} = \left[1 + \frac{\sqrt{V_f}}{2}A + \frac{\sqrt{V_f}}{2}(3 - V_f - \sqrt{V_f})B\right]\frac{(V_f + 0.3V_m)E_{22}^{f} + 0.7V_mE^{m}}{0.3E_{22}^{f} + 0.7E^{m}}, \tag{7.1}$$

$$K_{33}^{c} = \left\{1 - \frac{\sqrt{V_f}}{2}A\frac{\sigma_{u,c}^{m} - \sigma_{u,t}^{m}}{2\sigma_{u,c}^{m}} + \frac{B}{2(1-\sqrt{V_f})}\left[-V_f^{2}\left(1 - 2\left(\frac{\sigma_{u,c}^{m} - \sigma_{u,t}^{m}}{2\sigma_{u,c}^{m}}\right)^{2}\right) + \right.\right.$$
$$\left.\left.\frac{\left(\sigma_{u,c}^{m} + \sigma_{u,t}^{m}\right)V_f}{\sigma_{u,c}^{m}}\left(1 + \frac{\sigma_{u,c}^{m} - \sigma_{u,t}^{m}}{\sigma_{u,c}^{m}}\right) - \sqrt{V_f}\left(\frac{\sigma_{u,c}^{m} - \sigma_{u,t}^{m}}{\sigma_{u,c}^{m}} + 1 - 2\left(\frac{\sigma_{u,c}^{m} - \sigma_{u,t}^{m}}{2\sigma_{u,c}^{m}}\right)^{2}\right)\right]\right\}\times$$
$$\frac{(V_f + 0.3V_m)E_{22}^{f} + 0.7V_mE^{m}}{0.3E_{22}^{f} + 0.7E^{m}}, \tag{7.2}$$

$$A=\frac{2E_{22}^{f}E^{m}(\nu_{12}^{f})^{2}+E_{11}^{f}\{E^{m}(\nu_{23}^{f}-1)-E_{22}^{f}[2(\nu^{m})^{2}+\nu^{m}-1]\}}{E_{11}^{f}[E_{22}^{f}+E^{m}(1-\nu_{23}^{f})+E_{22}^{f}\nu^{m}]-2E_{22}^{f}E^{m}(\nu_{12}^{f})^{2}}, \tag{7.3}$$

$$B=\frac{E^{m}(1+\nu_{23}^{f})-E_{22}^{f}(1+\nu^{m})}{E_{22}^{f}[\nu^{m}+4(\nu^{m})^{2}-3]-E^{m}(1+\nu_{23}^{f})}, \tag{7.4}$$

$$K_{23}=2\sigma_{u,s}^{m}\sqrt{\frac{K_{22}^{t}K_{22}^{c}}{\sigma_{u,t}^{m}\sigma_{u,c}^{m}}}, \tag{7.5}$$

$$K_{12}=K_{13}=\left[1-V_{f}\frac{G_{12}^{f}-G^{m}}{G_{12}^{f}+G^{m}}\{W(V_{f})-\frac{1}{3}\}\right]\frac{(V_{f}+0.3V_{m})G_{12}^{f}+0.7V_{m}G^{m}}{0.3G_{12}^{f}+0.7G^{m}}, \tag{7.6}$$

$$W(V_{f})=\pi\sqrt{V_{f}}[\frac{1}{4V_{f}}-\frac{4}{128}-\frac{2}{512}V_{f}-\frac{5}{4096}V_{f}^{2}]. \tag{7.7}$$

$$\hat{K}_{33}^{t}=\mathrm{Re}\left\{e^{-2i\psi}M(be^{i\psi})(a^{2}/b-b)-e^{-i\psi}\left(N_{2}-N_{1}(\frac{a^{2}}{b}e^{-i\psi})\right)+\right.$$
$$\left.e^{-i\psi}(2+e^{-2i\psi})[N(be^{i\psi})-N_{3}]\right\}\frac{(V_{f}+0.3V_{m})E_{22}^{f}+0.7V_{m}E^{m}}{2(b-a)(0.3E_{22}^{f}+0.7E^{m})}, \tag{8.1}$$

$$N_{2}=aFe^{-i\psi}+akie^{i\psi},\quad N_{3}=Fae^{i\psi}+e^{-i\psi}ak, \tag{8.2}$$

$$N(z)=Fz+\frac{a^{2}k}{z}-(z-ae^{i\psi})^{0.5+i\lambda}(z-ae^{-i\psi})^{0.5-i\lambda}[(F-0.5)-\frac{D}{a^{2}z}], \tag{8.3}$$

$$N_{1}(z)=Fz+\frac{a^{2}k}{z}+\frac{1}{\xi}(z-ae^{i\psi})^{0.5+i\lambda}(z-ae^{-i\psi})^{0.5-i\lambda}[(F-0.5)-\frac{D}{a^{2}z}], \tag{8.4}$$

$$M(z)=F-\frac{a^{2}k}{z^{2}}-[(F-0.5)z+H+\frac{C}{z}+\frac{D}{z^{2}}]\chi(z), \tag{8.5}$$

$$F=\frac{1-(\cos\psi+2\lambda\sin\psi)\exp[2\lambda(\pi-\psi)]+(1-k)(1+4\lambda^{2})\sin^{2}\psi}{\frac{4}{k}-2-2(\cos\psi+2\lambda\sin\psi)\exp[2\lambda(\pi-\psi)]}, \tag{8.6}$$

$$H=a(\cos\psi+2\lambda\sin\psi)(0.5-F), \tag{8.7}$$

$$C=(k-1)(\cos\psi-2\lambda\sin\psi)a^{2}\exp[2\lambda(\psi-\pi)], \tag{8.8}$$

$$D=(1-k)a^{3}\exp[2\lambda(\psi-\pi)], \tag{8.9}$$

$$\chi(z)=(z-ae^{i\psi})^{-0.5+i\lambda}(z-ae^{-i\psi})^{-0.5-i\lambda}, \tag{8.10}$$

$$k=\frac{\mu_{1}(1+\kappa_{2})}{(1+\xi)(\mu_{1}+\kappa_{1}\mu_{2})},\ \lambda=-(\ln\xi)/(2\pi),\ \xi=(\mu_{2}+\kappa_{2}\mu_{1})/(\mu_{1}+\kappa_{1}\mu_{2}), \tag{8.11}$$

$$\kappa_{1}=3-4\nu^{m},\ \kappa_{2}=\frac{3-\nu_{23}^{f}-4\nu_{12}^{f}\nu_{21}^{f}}{1+\nu_{23}^{f}},\ \mu_{1}=\frac{E^{m}}{2(1+\nu^{m})},\ \mu_{2}=\frac{E_{22}^{f}}{2(1+\nu_{23}^{f})}, \tag{8.12}$$

$b=a/\sqrt{V_{f}}$, a is the radius of the fiber. (8.13)

In Eqs. (8.1)-(8.10), ψ is the half of the central angle corresponding to the fiber and matrix interface debonding, which is a solution to the following equations:

$$\mathrm{Re}\left\{\left(G_{0}-\frac{1}{k}-\frac{2(1-k)}{k\exp(i\varphi)}\exp[2\lambda(\psi-\pi)]\right)R(e^{i\varphi})\right\}_{\varphi=\psi-\gamma}=0, \tag{9}$$

$$G_{0}=\frac{1-(\cos\psi+2\lambda\sin\psi)\exp[2\lambda(\pi-\psi)]+(1-k)(1+4\lambda^{2})\sin^{2}\psi}{2-k-k(\cos\psi+2\lambda\sin\psi)\exp[2\lambda(\pi-\psi)]}, \tag{10.1}$$

$$R(\exp(i\varphi))=[\exp(i(\varphi))-e^{i\psi}]^{0.5+i\lambda}[\exp(i(\varphi))-e^{-i\psi}]^{0.5-i\lambda}\exp(-i(\varphi)), \tag{10.2}$$

$$\gamma = \frac{2\lambda(J_1^2 + J_2^2)}{J_1^2 + J_2^2 - 2J_2J_3}, \text{ if } \xi<1, \tag{10.3}$$

$$\gamma = -\frac{2\lambda(J_1^2 + J_2^2)}{J_1^2 + J_2^2 - 2J_2J_3}, \text{ if } \xi>1, \tag{10.4}$$

$$J_1 = kG_0 - 1 - 2(1-k)\xi \exp(2\lambda\psi)\cos(\psi), \tag{10.5}$$

$$J_2 = 2(1-k)\xi \exp(2\lambda\psi)\sin(\psi), \tag{10.6}$$

$$J_3 = 2(1-k)\xi \exp(2\lambda\psi)[J_1\cos(\psi) - J_2\sin(\psi)]/J_2. \tag{10.7}$$

It is noted that one should replace E_{22}^f by (1.01) E_{22}^f to guarantee that $\xi\neq1$. In Eqs. (7.2) and (7.5), $\sigma_{u,t}^m$, $\sigma_{u,c}^m$, and $\sigma_{u,s}^m$ are the original tensile, compressive, and shear strengths of the matrix, respectively. In Eq. (6), $\hat{\sigma}_e^m$ is the critical Mises stress at the interface debonding given by

$$\hat{\sigma}_e^m = \sqrt{(\hat{\sigma}_{11}^m)^2 + (K_{22}^t\hat{\sigma}_{22}^m)^2 - K_{22}^t\hat{\sigma}_{11}^m\hat{\sigma}_{22}^m}, \tag{11.1}$$

$$\hat{\sigma}_{22}^m = \frac{0.3E_{22}^f + 0.7E^m}{(V_f + 0.3V_m)E_{22}^f + 0.7V_mE^m}\hat{\sigma}_{22}^0, \tag{11.2}$$

$$\hat{\sigma}_{11}^m = \frac{V_fA_{12}}{(V_f + V_mA_{11})(V_f + V_mA_{22})}\hat{\sigma}_{22}^0, \tag{11.3}$$

$$\hat{\sigma}_{22}^0 = \frac{\hat{K}_{22}^tY}{\hat{K}_{22}^t - K_{22}^t} - \frac{(V_f + 0.3V_m)E_{22}^f + 0.7V_mE^m}{(0.3E_{22}^f + 0.7E^m)(\hat{K}_{22}^t - K_{22}^t)}\sigma_{u,t}^m. \tag{11.4}$$

Y is the transverse tensile strength of the UD composite made from the same fiber and matrix. $(\bar{\sigma}_e^m)_k$ and $(\bar{\sigma}_m^1)_k$ in Eq. (6) stand for the current Mises stress and the first principal stress calculated from the previous true stresses of the matrix, $\{\bar{\sigma}_{ij}^m\}_k = \{\bar{\sigma}_{11}^m, \bar{\sigma}_{22}^m, \bar{\sigma}_{33}^m, \bar{\sigma}_{23}^m, \bar{\sigma}_{13}^m, \bar{\sigma}_{12}^m\}_k^T$.

Following the reference [3], a delamination of the laminate is considered to initiate from the interlaminar stress components of the matrix. By using Tsai-Wu's criterion and ignoring the in-plane stress components, the initiation of a delamination takes place if the following condition is fulfilled

$$F_1(\bar{\sigma}_{33}^m)_{k+1}^2 + F_2[(\bar{\sigma}_{13}^m)_{k+1}^2 + (\bar{\sigma}_{23}^m)_{k+1}^2] + F_3(\bar{\sigma}_{33}^m)_{k+1} \geq 1 \tag{12.1}$$

where

$$F_1 = \frac{1}{\sigma_{u,t}^m\sigma_{u,c}^m}, F_2 = \frac{1}{(\sigma_{u,s}^m)^2}, F_3 = \frac{\sigma_{u,c}^m - \sigma_{u,t}^m}{\sigma_{u,t}^m\sigma_{u,c}^m}. \tag{12.2}$$

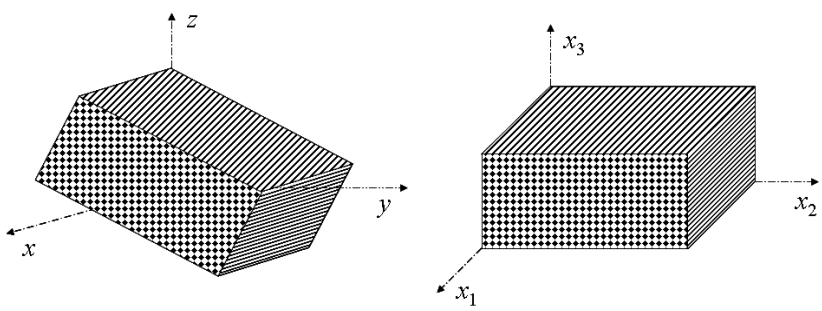

Figure 5: stress conversion form global coordinates to local coordinates

4 RESULTS AND DISCUSSION

As mentioned in the previous section, [$\pm\theta_n$]s (where $\theta=10^0,20^0,30^0$,n=1-5) was predicted to compare with the experimental results of reference [5] which provide the applied loads at delamination onset versus the ply thickness. Before analysis, the date that we need are the mechanical properties of fiber and matrix, which are summarized in **table 2**. The ply's thickness value is h_0=0.125mm.

Figure 6 show three interlaminar stresses distribution versus y in the matrix of -10 ply when [$\pm$10]s laminate delaminates. [$\pm10_n$]s laminates are known to delaminate at the +θ/-θ interface due to

the interlaminar shear stress of matrix. The interlaminar shear stresses of the matrix drastically decrease from the free edge when moving toward the plate's inside. It is noticed that the interlaminar stresses of the matrix are average stresses in a ply, which differ from the interlaminar stresses at the +θ/-θ interface. For example, $[\pm 10_2]$s laminates is consisted with four plies in the upper half of the laminate. The +θ and –θ ply, which are located above and below the +θ/-θ interface, are predicted through the approach to provide two predicted stresses. The average stress of these two predicted stresses is considered the applied stress at delamination onset. The same analytical process is also applicable to $[\pm 20_n]$s laminates and $[\pm 30_n]$s laminates. The predictions and the experiments of the $[\pm \theta_n]$s laminates are listed in **table 3** and reported in **figure 7**. Comparison of experimental theoretical results show a good agreement except for the [±10]s laminate.

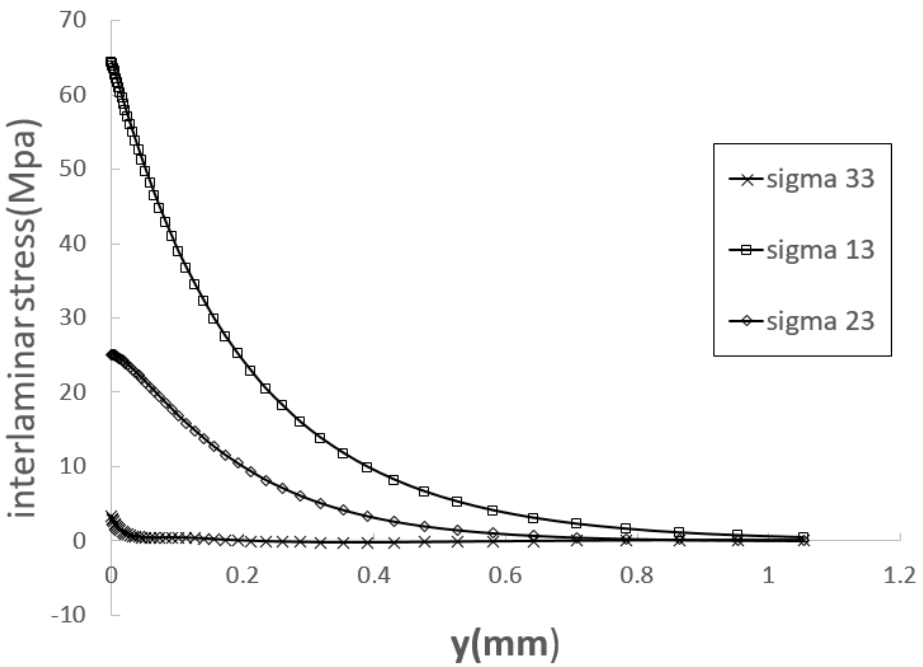

Figure 6: true interlaminar stress $\overline{\sigma}_{ij}^{III}$ of the matrix in -10 ply when [±10]s laminate delaminates

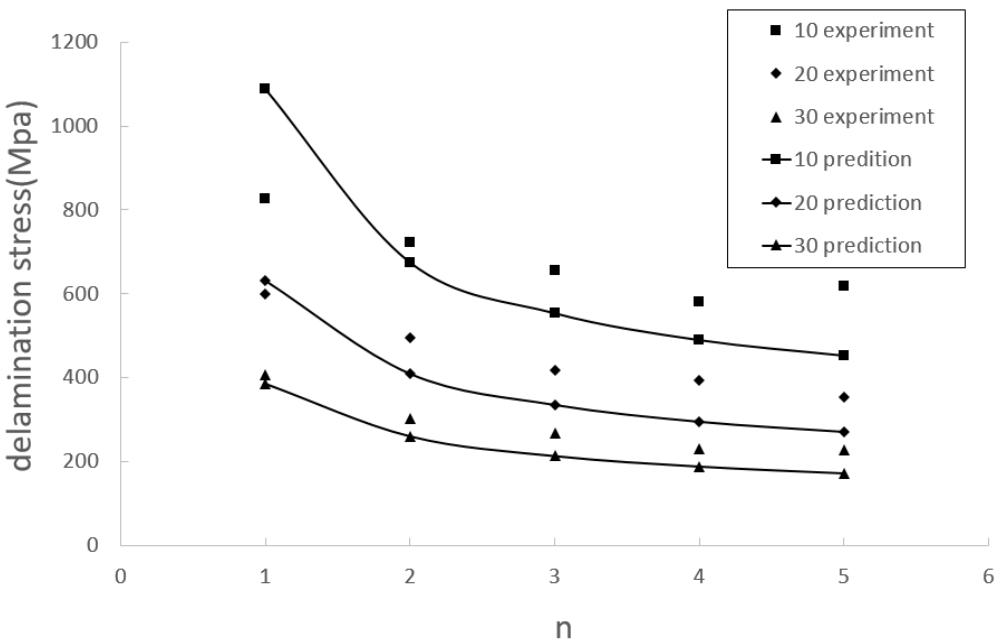

Figure 7: delamination prediction on T800/914 $[\pm \theta_n]$s laminate

	n	1	2	3	4	5
$[\pm 10_n]s$ (Mpa)	experiment	826	722	655	580	619
	prediction	1088	675	554	490	453
	deviation	31.72%	-6.51%	-15.42%	-15.52%	-26.82%
$[\pm 20_n]s$ (Mpa)	experiment	599	495	418	394	354
	prediction	631	410	336	296	272
	deviation	5.34%	-17.17%	-19.62%	-24.87%	-23.16%
$[\pm 30_n]s$ (Mpa)	experiment	406	304	269	232	227
	prediction	386	261	214	189	173
	deviation	-4.93%	-14.14%	-20.45%	-18.53%	-23.79%

Table 3:comparison of prediction and experiment results

5 CONCLUSIONS

In this paper, the authors present a micromechanical method to analyse the initiation of delamination at a free edge in $[\pm\theta_n]s$ laminate. The stress field of symmetrically laminated plates under an axial load is calculated by a finite element model. The interlaminar stress field in the vicinity of the free edge exhibits a stress singularity that can be solved by taking an average for the stresses of each lamina with respect to its thickness. And then combining the bridging model and the stress concentration factors, the stress of the matrix is determined. Finally a delamination criterion involving the stress and the original strength of the matrix is used to predict the applied load of delamination onset.

The results show that this approach is applicable for the $[\pm\theta_n]s$ laminates and reproduces the thickness and angle effects on the delamination observed experimentally. But only angle laminates appear in the paper. For the other delamination modes and the other materials, for example $[\pm 25_n/90_{n/2}]s$ laminates which delaminate due to the interlaminar normal stress, this method must be tested further.

ACKNOWLEDGEMENTS

Financial supports from the National Natural Science Foundation of China (Grant Nos. 11472192, 11272238) are acknowledged.

REFERENCES

[1] Pipes R B, Pagano N J. Interlaminar Stresses in Composite Laminates Under Uniform Axial Extension[J]. Journal of Composite Materials, 1970, 34(4):234-245.

[2] Pipes R B, Pagano N J. Interlaminar Stresses in Composite Laminates Under Uniform Axial Extension[J]. Journal of Composite Materials, 1970, 34(4):234-245.

[3] Kim R Y, Soni S R. Experimental and Analytical Studies On the Onset of Delamination in Laminated Composites[J]. Journal of Composite Materials, 1984, 18(1):70-80.

[4] Brewer J C, Lagace P A. Quadratic Stress Criterion for Initiation of Delamination [J]. Journal of Composite Materials, 1988, 22(12):1141-1155.

[5] Lorriot T, Marion G, Harry R, et al. Onset of free-edge delamination in composite laminates under tensile loading[J]. Composites Part B Engineering, 2003, 34(5):459-471.

[6] Wang A S D. Chapter 2 - Fracture Analysis of Interlaminar Cracking[M]// Composite Materials Series. 1989:69-109.

[7] Martin E, Leguillon D, Carrère N. A twofold strength and toughness criterion for the onset of free-edge shear delamination in angle-ply laminates[J]. International Journal of Solids & Structures, 2010, 47(9):1297-1305.

[8] Huang Z M, Xin L M. In situ strengths of matrix in a composite[J]. Acta Mechanica Sinica, 2017, 33(1):1-12.